Triple Coincidence $(e, \gamma 2e)$ Experiment for Simultaneous Electron Impact Ionization Excitation of Helium

G. Sakhelashvili,* A. Dorn, C. Höhr, and J. Ullrich
Max-Planck-Institut für Kernphysik, Saupfercheckweg 1, 69117 Heidelberg, Germany

A. S. Kheifets and J. Lower
Research School of Physical Sciences and Engineering, Australian National University, Canberra, ACT 0200, Australia

K. Bartschat
Department of Physics and Astronomy, Drake University, Des Moines, Iowa 50311, USA
(Received 4 February 2005; published 14 July 2005)

Simultaneous ionization and excitation of helium atoms by 500 eV electron impact is observed by a triple coincidence of an ionized slow electron, the recoiling He^+ ion, and the radiated vacuum ultraviolet photon ($\lambda \leq 30.4$ nm). Kinematically complete differential cross sections are presented for the $He^+(2p)^2P$ final ionic state, demonstrating the feasibility of a quantum mechanically complete experiment. The experimental data are compared to predictions from state-of-the-art numerical calculations. For large momentum transfers, a first-order treatment of the projectile-target interaction can reproduce the experimental angular dependence, but a second-order treatment is required to obtain consistent magnitudes.

DOI: 10.1103/PhysRevLett.95.033201 PACS numbers: 34.80.Dp, 34.80.Pa

Understanding of correlated quantum dynamics in few- and many-body systems is a challenging task with implications going far beyond pure physics. Questions range from mechanisms of high-T_c superconductivity or spintronics in solid-state physics to the femtochemistry of tunneling proton migration in water and time-dependent molecular bond formation or breaking, and even to the biology of protein folding dynamics or DNA double-strand break reactions, which occur through negative-ion resonances in collisions with low-energy electrons.

The investigation of fundamental atomic reactions plays a central, benchmarking role in this context, since the dominating Coulomb interaction is known exactly, the number of actively participating particles m can be fully controlled, and the initial and final quantum states may be completely determined for reactions of limited complexity. For over 30 years, efforts have concentrated on exploring the simplest nontrivial system involving two electrons and one recoiling ion ($m = 3$) by kinematically complete experiments, in which the final-state momentum vectors of all particles are determined. Numerous studies of the electron-impact single ionization, $(e, 2e)$, of atomic hydrogen performed since 1979 [1] or photo-double-ionization, $(\gamma, 2e)$, of helium since 1993 (see Ref. [2] for a review) have tremendously advanced our understanding of the dynamical three-body problem. In particular cases, e.g., for light particle impact at low impact energies, it even has been solved exactly computationally in 1999 [3].

However, troubling discrepancies between experimental results and predictions of all state-of-the-art theories were recently observed in four-body systems with essentially three active particles, such as single ionization of helium by fast ion impact [4]. This statement also holds for the first kinematically complete experiments on electron-impact double ionization of helium ($m = 4$) [5–7], demonstrating impressively our difficulties in understanding just four Coulomb-interacting quantum particles. Therefore, these and other fundamental collision problems involving the helium target, as, e.g., double excitation [8] or the process investigated in the present work, ionization of one electron with simultaneous excitation of the other one,

$$e_0(\boldsymbol{k}_0) + \mathrm{He}(1s^2)^1S \rightarrow \mathrm{He}^+(2\ell)^2L(\boldsymbol{k}_R) + e_a(\boldsymbol{k}_a) + e_b(\boldsymbol{k}_b), \quad (1)$$

play a decisive role in advancing to $m = 4$. Here, the projectile with momentum $\boldsymbol{k}_0$ is scattered to a momentum state $\boldsymbol{k}_a$, thereby transferring energy and momentum $\boldsymbol{q} \equiv \boldsymbol{k}_0 - \boldsymbol{k}_a$ to the target atom. One electron with momentum $\boldsymbol{k}_b$ is emitted and an excited target ion is left, recoiling with momentum $\boldsymbol{k}_R$. The investigation of this reaction in a so-called $(e, \gamma 2e)$ experiment bears the chance to perform a "quantum mechanically complete experiment," the Holy Grail of quantum dynamics, by measuring, in coincidence, the two outgoing electrons and the angular distribution or the polarization of the fluorescence photon in the radiative decay $He^+(2p)^2P \rightarrow He^+(1s)^2S + h\nu$ with a photon wavelength ($\lambda = 30.4$ nm) [9–11].

Such a triple-coincidence experiment has not been feasible to date due to the discouragingly low detection efficiencies of traditional multicoincidence techniques. Pioneering double-coincidence studies performed for $He^+(n = 2)$ states can be grouped into $(e, 2e)$ [12–14] and $(e, \gamma e)$ [15,16] investigations, either summing the contributions from the $2s$ and $2p$ states of He^+ or leaving the collision kinematics undefined by not detecting the second electron.

In this Letter, we report on a kinematically complete triple-coincidence $(e, \gamma 2e)$ experiment performed by exploiting novel many-particle imaging technologies for the ions and electrons in a "reaction microscope" [17] combined with a large solid-angle detection of fluorescence photons. The apparatus (see Fig. 1) is located at the Max-Planck-Institut für Kernphysik in Heidelberg. It is dedicated to and specially designed for the investigation of electron scattering processes [18]. The spectrometer has been extended by two large-area (80 mm diameter) multichannel plate photon detectors positioned at 90° with respect to the incoming projectile beam. They cover 10% of the full solid angle and reach a detection efficiency of about 10% for the photon energies of interest. The projectile electron beam ($E_0 = 500$ eV) is crossed with a supersonic helium jet (1 mm diameter, 10^{12} atoms/cm^3). The low-energy ($E_b < 12.5$ eV) ejected electron and the recoiling He^+ target ion are projected by homogeneous electric (1.2 V/cm) and magnetic (6 G) fields with a 4π solid angle onto position- and time-sensitive microchannel plate detectors (40% detection efficiency each). Thus, an overall three-particle detection efficiency of about 0.16% is achieved.

The ion and electron longitudinal momentum components ($k_\parallel = k_z$), along the z axis in Fig. 1, are deduced from the times of flight (TOF), while the transverse momentum components (k_x, k_y) are obtained from the impact positions on the detectors in the xy plane and the TOFs [17,19]. Thus, measuring the momentum vectors of the fragments ($\boldsymbol{k}_b$, $\boldsymbol{k}_R$) in coincidence allows us to deduce both the momentum of the scattered electron $\boldsymbol{k}_a = \boldsymbol{k}_0 - \boldsymbol{k}_b - \boldsymbol{k}_R$ and the momentum transfer $\boldsymbol{q} = \boldsymbol{k}_0 - \boldsymbol{k}_a = \boldsymbol{k}_b + \boldsymbol{k}_R$.

The main experimental challenge is posed by huge background signal rates. These, in combination with small detection efficiencies, were ultimately responsible for the failure of earlier attempts to perform $(e, \gamma 2e)$ measurements. Background events include charged fragments produced in singly ionizing collisions and intense vacuum ultraviolet photons emitted by neutral helium after collisional excitation. Each of the corresponding processes are about 2 orders of magnitude more likely than the one of interest, i.e., simultaneous ionization excitation. Since the number of random coincidences is proportional to the product of the three individual detector count rates and thus to the third power of the projectile beam current I, while the number of true coincidences only scales linearly with I, the true events will be easily buried for high projectile beam currents. Hence, the large detection efficiencies and the solid angles reached in our reaction microscope, which allow for projectile beam currents as small as $I = 60$ pA, are crucial for the feasibility of the experiment. In addition, we can use energy and momentum conservation to further discriminate against random coincidences.

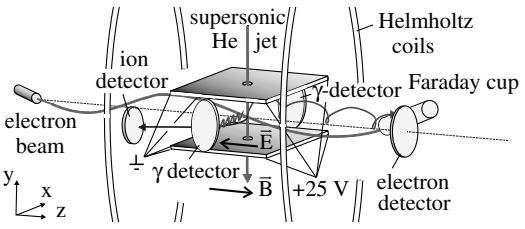

FIG. 1. Schematic of the experimental setup.

The experiment was operated using a continuous electron beam. A detected photon served as the trigger to tag the desired $(e, \gamma 2e)$ event by starting [with negligible delay due to the excited state lifetime $\tau(2p) = 0.6$ ns] the TOF measurement for the electrons (TOF ≈ 200 ns) and the ions (TOF ≈ 17 μs). In a two-dimensional triple-coincidence spectrum (see Fig. 2), random coincidences were identified by exploiting the increased energy loss (Q value) of the true ionization-excitation reaction ($Q \geq 65.4$ eV for $n \geq 2$) compared to those of false ionization-only ($Q = 24.6$ eV) events. The difference in the TOF between the photon and the electron, $\Delta_{\mathrm{TOF}}(\gamma - e^-)$, essentially the electron TOF and thus its longitudinal momentum, is plotted versus $\Delta_{\mathrm{TOF}}(e^- - \mathrm{He}^+)$ between the electron and the He^+ recoil ion. Note that $\Delta_{\mathrm{TOF}}(e^- - \mathrm{He}^+)$ is proportional to the sum of the longitudinal electron ($k_{b\parallel}$) and ion ($k_{R\parallel}$) momenta, from which the Q value can be obtained [19]:

$$Q/v + E_b/v = k_{R\parallel} + k_{b\parallel} \propto \Delta_{\mathrm{TOF}}(e^- - \mathrm{He}^+). \qquad (2)$$

Here $v = 6$ is the projectile velocity (in atomic units) for $E_0 = 500$ eV. Since all detected electrons have energies $E_b < 15$ eV, the contribution from $E_b/v < 0.1$ a.u. may be neglected. (It is actually taken into account in the detailed analysis.) The abscissa of Fig. 2, $\Delta_{\mathrm{TOF}}(e^- - \mathrm{He}^+)$, then approximately represents the Q value of the reaction.

Three features are observed in Fig. 2: (i) A band along a Q value close to 24.6 eV, corresponding to single ionization. The random photon TOF shows no correlation, thereby indicating pure $(e, 2e)$ events. (ii) A sharp peak

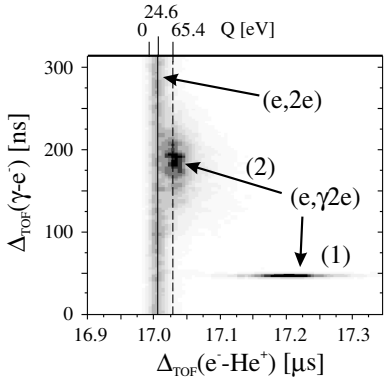

FIG. 2. Triple-coincidence timing spectrum. The number of counts is plotted as function of the TOF differences $\Delta_{\mathrm{TOF}}(e^- - \mathrm{He}^+)$ and $\Delta_{\mathrm{TOF}}(\gamma - e^-)$. See text for details.

(1) in $\Delta_{\mathrm{TOF}}(\gamma - e^-)$ for very short flight times of the electron corresponding to photons coincident with fast projectile electrons scattered onto the electron detector. The He^+ recoil ion is coincident as well, showing a broad pattern due to its momentum distribution. Since the slow electron is not detected here, the ion momentum is not compensated for and the Q value cannot be derived. (iii) Another peak (2) at about the correct Q value, which is broad in the electron TOF due to the momentum distribution of the slow electron e_b. The correct Q value and the true photon-electron coincidence peak provide the unique signature of a true triple-coincidence $(e, \gamma 2e)$ event. The Q-value resolution in the present experiment is not sufficient to discriminate between excitation into different n shells of $He^+(np)^2P$ states, but we expect this to be possible in the future. Finally, since the band of false $(e, 2e)$ contributions is not fully separated from the true coincidences, a background spectrum was generated for each cross section presented and subtracted.

Figure 3 shows fully differential cross sections $d^3\sigma/d\Omega_a d\Omega_b dE_b$ for the incident energy $E_0 = 500$ eV, two different energies of the ionized electron ($E_b = 3 \pm 1.5$ eV and 10 ± 2 eV), and two different momentum transfers ($|\boldsymbol{q}| = 0.6 \pm 0.1$ a.u. and $|\boldsymbol{q}| = 2.0 \pm 0.4$ a.u.). We have chosen a coplanar scattering geometry; i.e., only electron emission into the projectile scattering plane is considered, allowing for an angular acceptance range of $\pm 20°$. The angular emission patterns of the ejected electron e_b are in striking contrast to typical $(e, 2e)$ spectra under similar kinematical conditions. Only at $E_b = 10$ eV and $|\boldsymbol{q}| = 2$ a.u. are there indications of the binary and recoil peaks, i.e., cross section maxima for emission into the $+\boldsymbol{q}$ and $-\boldsymbol{q}$ directions. The complexity of the other spectra originates from the many-body character of the collision. While the $(e, 2e)$ process is dominated by a single interaction of the projectile with the ejected electron, $(e, \gamma 2e)$ requires additional interactions of the projectile or the ejected electron with the remaining target electron and/or strong correlations in the initial bound state.

In order to shed more light on this complex process, the experimental results are compared with two different theoretical predictions. Both models treat the interaction between the fast projectile and the target perturbatively, while the ejected-electron–residual-ion interaction (effectively electron scattering from He^+ with appropriate boundary conditions for ionization) is handled via convergent multichannel expansions using momentum-space close-coupling (CCC) or a configuration-space R matrix with pseudostates (RMPS) approach. These methods yield nearly identical first-order results [20], but they differ in the extent to which second-order effects in the projectile-target interaction are incorporated. So far the CCC method accounts only for dipole interactions in second order [21], while the RMPS implementation includes monopole, dipole, and quadrupole terms [22,23]. Consequently, the second-order CCC approach is currently limited to small momentum transfers.

The calculations were performed for the ionic $He^+(2p)^2P$ state alone. Independent experimental observations indicate that excitation to $He^+(3p)^2P$ amounts to about 10%, and all higher excitations to not more than another 10% of the $He^+(2p)^2P$ cross section [24]. It is important to note that the experimental data in the panels of Fig. 3 are relative but cross normalized to each other. In order to put them on an absolute scale, we scaled *all* raw data with a *single* common factor. That factor was deter-

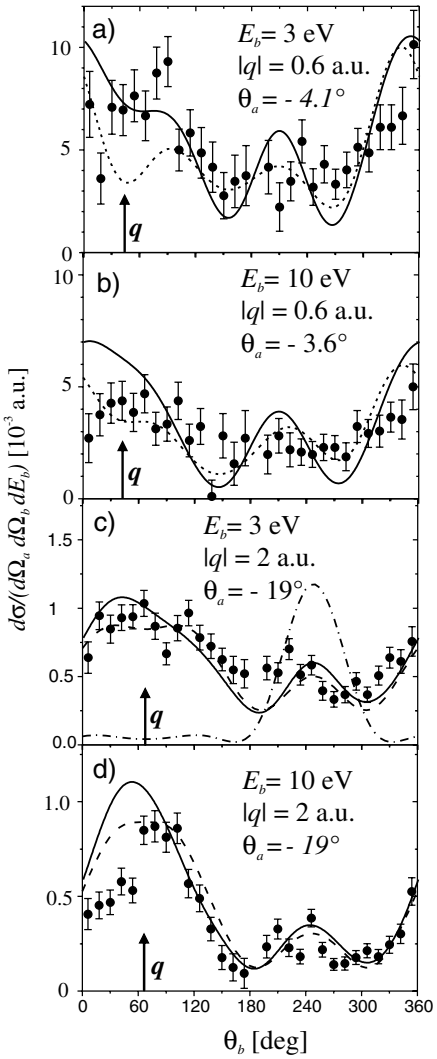

FIG. 3. Triple differential cross sections $d^3\sigma/(d\Omega_a d\Omega_b dE_b)$ at $E_0 = 500$ eV as a function of the slow-electron emission angle θ_b, measured with respect to the projectile beam forward direction. The energies E_b, the momentum transfers $|\boldsymbol{q}|$, and the projectile scattering angles θ_a are indicated in the diagrams. Solid lines: second-Born RMPS calculation. Dotted lines: second-Born CCC calculation. Dashed line in (c),(d): first-Born CCC calculation, multiplied by 2.5. Dash-dotted line in (c): first-Born CCC calculation for the $He^+(2s)^2S$ final ionic state.

mined by visually fitting the magnitude of the second-order RMPS results at $|\boldsymbol{q}| = 2$ a.u. and $E_b = 3$ eV, where the agreement in shape is good and the experimental error bars are relatively small.

At large momentum transfers, the second-order RMPS and the first-order CCC (and RMPS, although not shown) results agree very well with each other and with experiment as far as the *shape* of the curves is concerned. Thus, the symmetry of the angular distribution pattern with respect to the momentum-transfer direction (a signature of a first-Born model) is essentially maintained in the second-order result. On the other hand, the first-order CCC result had to be multiplied by 2.5 to obtain the same magnitude. This indicates a strong second-order contribution, which seems to manifest itself mainly in the magnitude of the cross section and leads only to small angular shifts of the peaks as it is observed for $E_b = 10$ eV.

At small momentum transfer, $|\boldsymbol{q}| = 0.6$ a.u., the second-Born CCC results agree with the R-matrix predictions for the magnitude of the cross section, but now the shapes are very different. At $E_b = 10$ eV, where resonances in the $e - \mathrm{He}^+$ collision problem make the comparison difficult [25], none of the second-order models reproduces the experimental data very well.

On the other hand, at $E_b = 3$ eV the second-order RMPS model is in satisfactory agreement with the experimental data, in particular, in the angular range 30°–150°. In contrast to $|\boldsymbol{q}| = 2.0$ a.u., the symmetry of the angular emission pattern with respect to the momentum-transfer axis is now clearly broken, thereby demonstrating the importance of high-order contributions.

Finally, the strong influence of the angular momentum of the final ionic state on the emission pattern is seen from the dash-dotted line in Fig. 3(c). It shows the first-Born CCC cross section for the energetically degenerate $\mathrm{He}^+(2s)^2S$ final state. With a pronounced recoil peak, the shape of this curve is very different from that for the $\mathrm{He}^+(2p)^2P$ final state. In principle, coherence effects between the two states may be revealed through Stark mixing [11], but this is not yet possible in our setup.

We have reported a successful triple-coincidence experiment for simultaneous ionization excitation of helium. This is a prototype reaction for the dynamical four-body Coulomb quantum problem. By detection of the radiated vacuum ultraviolet photons, the n^2P final ionic states could be separated from the n^2S states. Comparison with state-of-the-art numerical calculations revealed the importance of accounting for second-order effects in the projectile-target interaction. To stimulate and assess the quality of further theoretical efforts, more experimental benchmark data are urgently needed. In turn, by revealing potentially interesting kinematical scenarios for these very time-consuming studies, numerical calculations are helpful as a guide to experimentalists. The current experiment also demonstrates the feasibility of the ''complete experiment'' for simultaneous ionization excitation.

This work was supported, in part, by the Australian Research Council (J. L. and A. S. K.) and the United States National Science Foundation (K. B.).

*Present address: Tbilisi State University, Chavchavadze Avenue 3, 0179 Tbilisi, Georgia.

[1] E. Weigold, C. J. Noble, S. T. Hood, and I. Fuss, J. Phys. B **12**, 291 (1979).
[2] J. S. Briggs and V. Schmidt, J. Phys. B **33**, R1 (2000).
[3] T. N. Rescigno, M. Baertschy, W. A. Isaacs, and C. W. McCurdy, Science **286**, 2474 (1999).
[4] M. Schulz *et al.*, Nature (London) **422**, 48 (2003).
[5] I. Taouil, A. Lahmam-Bennani, A. Duguet, and L. Avaldi, Phys. Rev. Lett. **81**, 4600 (1998).
[6] A. Dorn *et al.*, Phys. Rev. Lett. **82**, 2496 (1999).
[7] A. Dorn *et al.*, Phys. Rev. Lett. **86**, 3755 (2001).
[8] W. T. Htwe, T. Vajnai, M. Barnhart, A. D. Gaus, and M. Schulz, Phys. Rev. Lett. **73**, 1348 (1994).
[9] V. V. Balashov and I. V. Bodrenko, J. Phys. B **32**, L687 (1999).
[10] N. Andersen and K. Bartschat, *Polarization, Alignment, and Orientation in Atomic Collisions* (Springer, New York, 2001).
[11] N. Andersen and K. Bartschat, J. Phys. B **37**, 3809 (2004).
[12] C. Dupré, A. Lahmam-Bennani, A. Duguet, F. Mota-Furtado, P. F. O'Mahony, and C. Dal Cappello, J. Phys. B **25**, 259 (1992).
[13] L. Avaldi, R. Camilloni, R. Multari, G. Stefani, O. Robaux, R. J. Tweed, and G. N. Vien, J. Phys. B **31**, 2981 (1998).
[14] B. Rouvellou, S. Rioual, A. Pochat, R. J. Tweed, J. Langlois, G. N. Vien, and O. Robaux, J. Phys. B **33**, L599 (2000).
[15] P. A. Hayes and J. F. Williams, Phys. Rev. Lett. **77**, 3098 (1996).
[16] M. Dogan, A. Crowe, K. Bartschat, and P. J. Marchalant, J. Phys. B **31**, 1611 (1998).
[17] R. Moshammer, M. Unverzagt, W. Schmitt, J. Ullrich, and H. Schmidt-Böcking, Nucl. Instrum. Methods Phys. Res., Sect. B **108**, 425 (1996).
[18] A. Dorn *et al.*, Phys. Rev. A **65**, 032709 (2002).
[19] J. Ullrich, R. Moshammer, A. Dorn, R. Dörner, L. Ph. H. Schmidt, and H. Schmidt-Böcking, Rep. Prog. Phys. **66**, 1463 (2003).
[20] A. S. Kheifets, I. Bray, and K. Bartschat, J. Phys. B **32**, L433 (1999).
[21] A. S. Kheifets, Phys. Rev. A **69**, 32 712 (2004).
[22] R. H. G. Reid, K. Bartschat, and A. Raeker, J. Phys. B **31**, 563 (1998); **33**, 5261(E) (2000).
[23] Y. Fang and K. Bartschat, J. Phys. B **34**, 2747 (2001).
[24] J. Lower *et al.*, in *Electron and Photon Impact Ionisation and Related Topics—2002*, Proceedings of the International Conference on Electron and Photon Impact Ionisation and Related Topics, edited by L. U. Ancarani, IOP Conf. Proc. No. 172 (Institute of Physics and Physical Society, London, 2003), p. 31.
[25] Y. Fang and K. Bartschat, Phys. Rev. A **64**, 020701 (2001).